



Communication

# Hemodynamic aspects of the Budd–Chiari syndrome of the liver: A computational model study

Harvey Ho<sup>a,\*</sup>, Chen Qiu<sup>b</sup><sup>a</sup>Bioengineering Institute, The University of Auckland, Auckland 1010, New Zealand<sup>b</sup>Department of Physiology, School of Medical Sciences, The University of Auckland, Auckland 1010, New Zealand

## ARTICLE INFO

## Article history:

Received 23 May 2018  
 Revised 16 April 2019  
 Accepted 26 April 2019

## Keywords:

Budd–Chiari syndrome  
 Liver  
 Hepatic circulation  
 Electrical analog

## ABSTRACT

Budd–Chiari syndrome (BCS) is a rare liver disease characterised by the obstruction of draining hepatic veins, and subsequent reduced blood return to the heart. Although many clinical BCS studies have been reported, few studies have quantified the associated changes that occur in the entire hepatic circulation. In this communication, we present an electrical analog model of the hepatic circulation that incorporates the Hepatic Arterial Buffer Response (HABR) mechanism in both the left and right lobes. Using this model we can simulate the hepatic flow under both normal and acute BCS conditions. The model can capture subtle features in the hepatic circulation, such as reduced total portal flow but increased arterial flow under BCS. This observation was previously reported in literature and may have clinical implications. As such, we suggest the presented model could be used for the analysis of systematic haemodynamic changes of BCS and therefore may be useful in supporting clinical interventions.

© 2019 IPEM. Published by Elsevier Ltd. All rights reserved.

## 1. Introduction

The liver has extensive vasculatures to serve its primary roles of oxygen and nutrient delivery, metabolism and drug detoxification. In brief, the liver vasculature is composed of a dual supply system: a portal venous (PV) network and a hepatic arterial (HA) network, which are both drained by a hepatic venous (HV) network consisting of left, middle and right branches (Fig. 1, inset (a)) [1]. The liver parenchyma may be divided into eight segments according to the Couinaud classification [2]. In this classification, the middle hepatic vein (MHV) is used to split left (segments II–IV) and right lobes (segments V–VIII), hence the MHV may drain blood flow from both left and right lobes.

Budd–Chiari syndrome (BCS) is a rare liver disease that is characterised by obstruction of HVs, and thereby leads to the poor blood drainage [3,4]. BCS can be further classified into primary BCS which is caused by thrombosis in the HVs, or secondary BCS which is due to invasion or compression of HV tracts from tumours [3,5]. The manifesting flow congestion causes ascites, stomach bloating, abdominal pain and hepatomegaly (swollen liver) [1]. Clinical treatments aim to alleviate HV obstruction and portal hypertension via a graded treatment approach including anti-coagulation medication, endovascular therapy, and surgical shunting [1].

Hemodynamic data have been rarely collected from BCS patients (see, for example, Cazals-Hatem et al. [6]). However, few quantitative studies have examined changes that occur in the hepatic circulation under BCS. The aim of this work is to build a computer model which is not overly complicated, yet can still capture major hemodynamic changes resulting from BCS. These findings may have clinical relevance in terms of pre- and post-surgical intervention.

## 2. Methods

## 2.1. A baseline electrical analog model

In a previous study by Ho et al. [7] an electrical analog model was used to simulate the Hepatic Arterial Buffer Response (HABR) effect, whereby the changes in HA flow counteracts that of the PV flow [8]. The analog model of Ho et al. [7] however does not differentiate blood flow into the left and right lobes, which is necessary in characterising the BCS condition, as the incidence of occlusion in the right HV is four times higher than the left HV [9].

In order to more accurately represent the BCS condition, we expanded the electric analog circuit by separating the PV and HA into a lumped second generation to represent left and right branches. The same process was applied to the HV, where the second generation is constructed of left, middle and right trunks, as shown in Figure 1, inset (a). In the improved model, each vasculature

\* Corresponding author.

E-mail address: [harvey.ho@auckland.ac.nz](mailto:harvey.ho@auckland.ac.nz) (H. Ho).

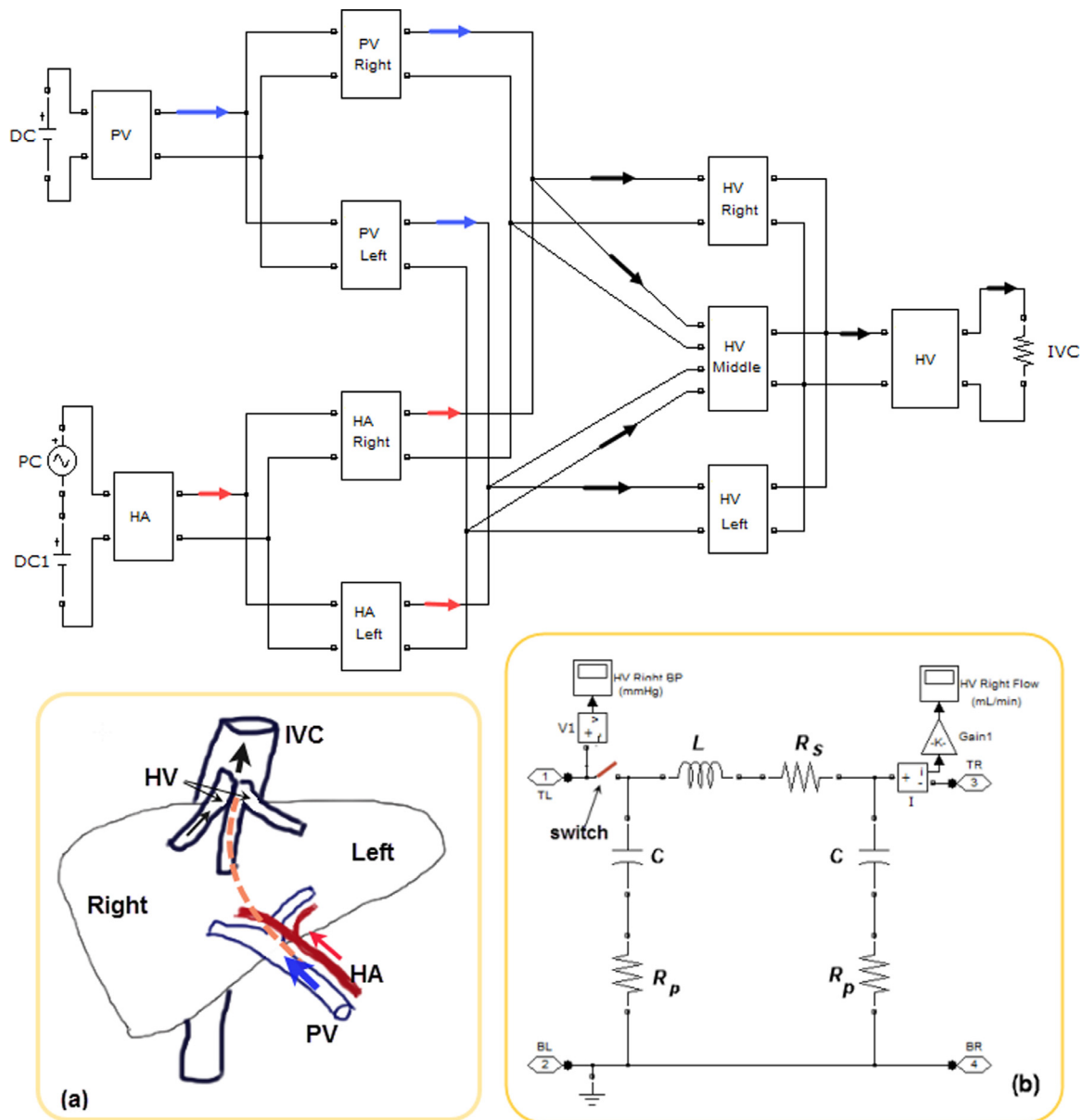


**Figure 1.** Schema of the electrical analog model representing three vasculatures (PV, HV, and HA) to their second generation. (a) Vascular anatomy of the liver, the dotted line splits the liver into left and right lobes; (b) The pi-filter for the right HV, note that a switch was introduced to occlude the segment. Gain1 in inset (b) is the intermediary in unit conversion from current to flow rate. Abbreviations: HA – hepatic artery; PV – Portal vein; HV – hepatic vein; IVC – inferior vena cava.

is represented by a single pi-filter (one is shown in inset (b) of Fig. 1). Non-linear resistors were used for HAs to simulate the HABR effects [7].

The circuit contains 30 resistors, 20 capacitors, and 10 inductors in total. The parameters attributed to the electronic elements were taken from two previous studies [7,11]. In brief, each pi-filter contains four parameters ( $R_s$ ,  $R_p$ ,  $C$  and  $L$ , as indicated in Fig. 1(b)) that represent resistance to blood flow, vessel viscoelasticity and compliance, blood inertial force, respectively. These are calculated from the data provided in Debbaut et al. [10]. Furthermore, the model parameters are calibrated by evaluating flow distribution into the left and right lobes as per the mass volume ratio [11] since the model in Debbaut et al. [10] does not differentiate left and right branches. The nominal values for electric analog components and conversion coefficients to blood flow are provided in the Supplementary file.

The model was implemented using the SimPowerSystem toolbox in SimuLink of Matlab. The Matlab differential equation solver,

ode32, was used for the numerical computation of the electric analog model. An arterial pressure waveform ranging between 80 and 120 mmHg and a PV pressure of 8 mmHg (Fig. 2(a)) were the imposed boundary conditions. A fully-annotated circuit diagram is provided in the on-line supplement.

### 2.2. Electrical analog model for BCS

Under BCS, the HV lumen is drastically reduced or even occluded, as such the return of blood from the liver to the heart is difficult. From a hemodynamic point of view, this is equivalent to a much higher resistance to blood flow which could be simulated by a resistor of much increased resistance value or an electrical switch. We selected the case of acute right HV occlusion among various BCS scenarios due to its high prevalence [9]. According to a clinical study of 101 BCS patients [9], right HV occlusion occurred in 82% (83 of 101) of the patients, and is thus of most clinical interest.

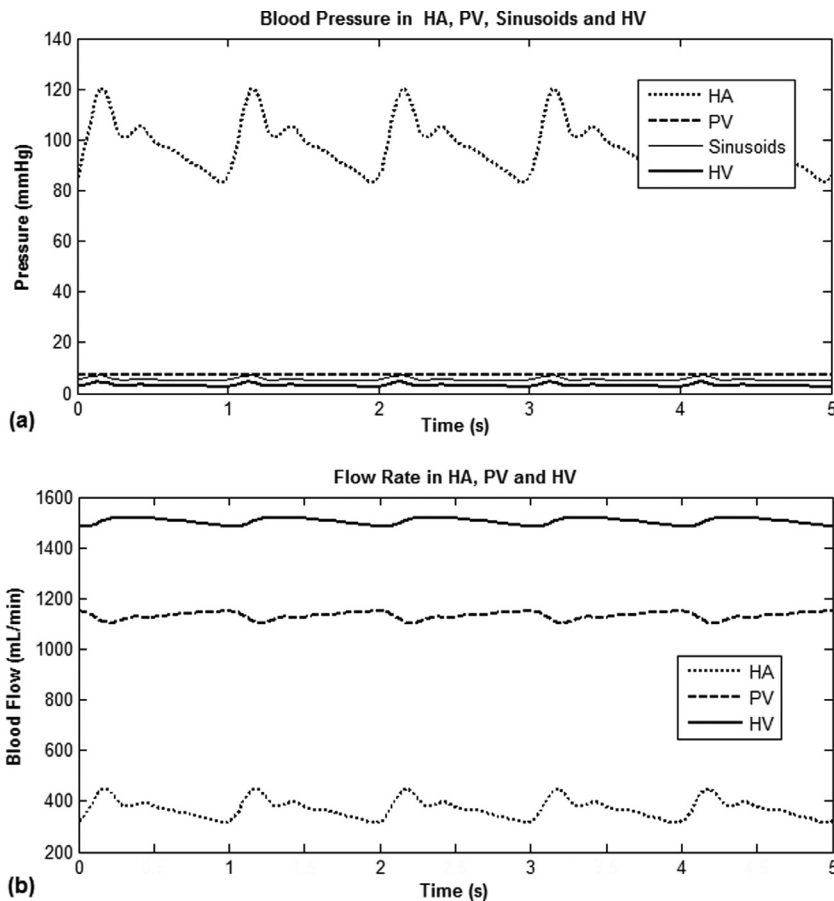


**Figure 2.** Nominal pressure and flow simulation in HA, PV and HV from the baseline model: (a) the sinusoidal pressure and hepatic vein pressure were 3, and 5–7 mmHg, respectively; (b) portal flow contributes to 75% of the hepatic circulation.

In order to simulate this flow occlusion, a switch was introduced in the circuit to disconnect the right HV from the main HV trunk (Fig. 1 inset (b)). Occlusion of other HV locations can be handled in a similar fashion.

For model validation, the simulation results of baseline model representing a healthy adult subject are compared with flow and pressure data obtained from the literature [8,12]. For the BCS simulation, we refer to the qualitative descriptions available in the literature (e.g., Cazals-Hatem et al. [6]).

### 3. Results

#### 3.1. Baseline model

A simulation for the hepatic circulation was first made using the baseline model to ensure that the values were physiologically relevant. The results are shown in Figures 2 and 3. The simulated sinusoidal pressure and hepatic vein pressure were 7–8 mmHg and 3–5 mmHg respectively, whilst the flow rates in the PV, HA and HV networks were 1125 mL/min, 375 mL/min and 1500 mL/min, respectively. This indicates that portal flow contributes to 75% (=1125 mL/1500 mL) of the total hepatic flow. These flow and pressure data are consistent with that reported elsewhere [8,12].

Figure 3 shows the flow distribution in the left and right PV and HA branches. In general, the left HA and PV supply about 35% of the total hepatic flow because the left lobe is smaller than the right lobe and thus necessitates a lower flow rate to maintain homeostasis of the liver hepatocytes [12].

The HV drainage is more complicated because the middle HV drains both left and right lobes. Furthermore there are significant

HV variations among different subjects. Without losing generality, we assumed that the drainage through the right, middle and left HVs were ~700 mL, ~500 mL and ~300 mL, respectively based on the average mass volume percentage [11].

#### 3.2. Right HV obstruction model

Having established a baseline for the hepatic flow, we examined the haemodynamics in the presence of BCS using the methods described in Section 2.2. We hypothesised that acute right HV occlusion would cause substantial flow redistribution in the liver due to the larger volume of the right lobe. A direct consequence of the syndrome is the accumulation of blood in the sinusoids and portal vein in the right lobe, which could cause sinusoidal and portal hypertension [1,3]. However, we assumed that the accumulated blood in the large right lobe may still be drained through anastomosis into the middle and left HVs, which are patent. Therefore the overall hepatic flow rate does not change drastically as observed in Figure 4, where a complementary increase in flow is observed in the middle and left HV that appears to complement the occlusion of the right HV.

More specifically, a simulation was made for 60 cardiac cycles (1 s per cycle), assuming the switch on the right HV network was turned off at 30 s. The simulation results are shown in Figures 4 and 5. In Figure 4, the flow in the right HV was zero as it was occluded. However, there were substantial flow increases in both middle (~65%) and left HVs (~77%) to drain the redirected flow from the right lobe.

It can be seen from Figure 5(b) that the right PV flow reduces and is drained by the middle HVs (Fig. 4). On the other

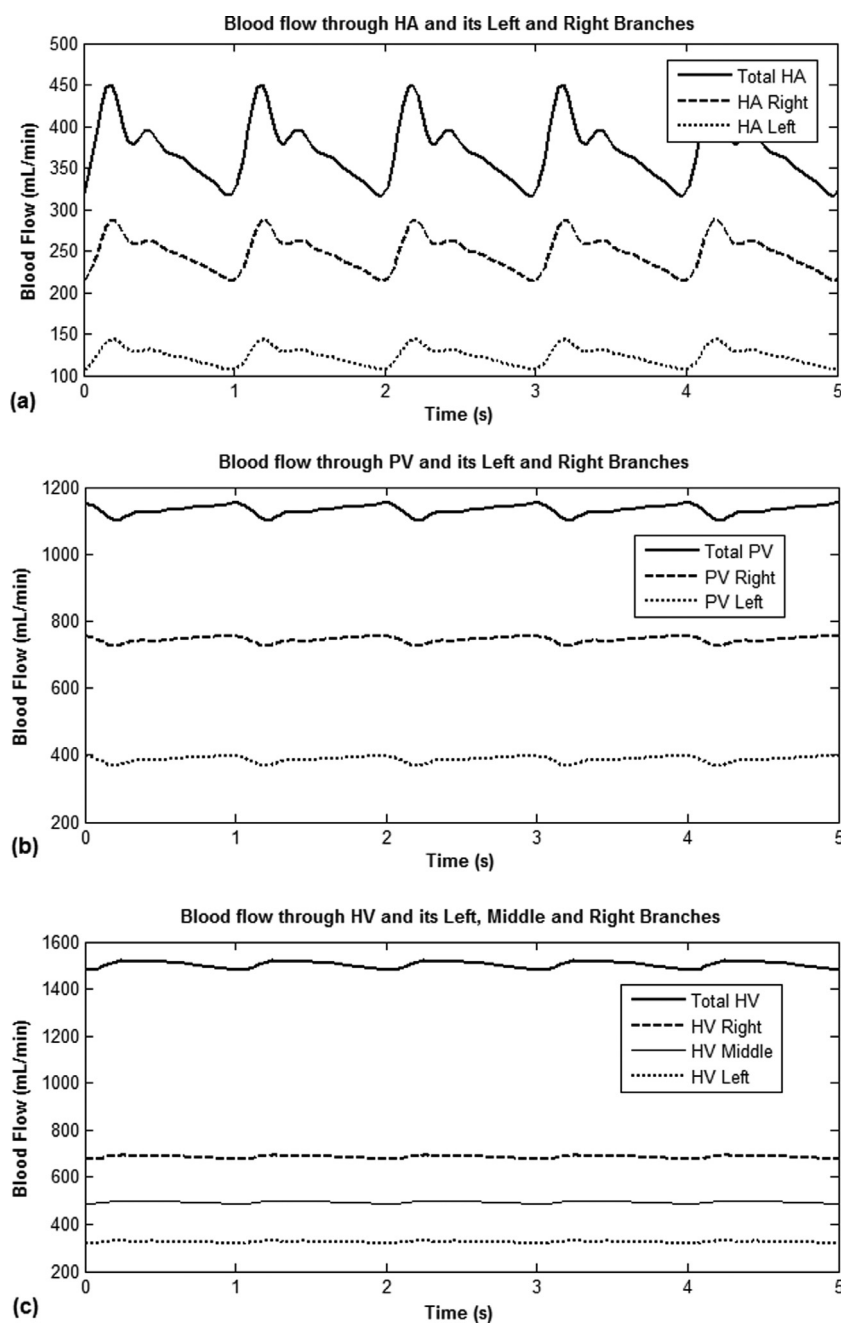


**Figure 3.** Nominal flow simulation in right, left branches of (a) HA, (b) PV, and (c) drainage in left, middle and right HV.

hand, the right HA flow increases due to HABR (Fig. 5(a)). This interesting phenomenon was also observed in BCS patients to receive liver transplantation [6]. Meanwhile, the flow in the left PV increases (by ~50% to 580 mL) to maintain the total PV flow (Fig. 5(d)). However, there was slight decrease (6%, from 1150 to 1080 mL/min) of total portal flow after right HV occlusion. This is caused by a higher resistance in the smaller vascular bed that is required to drain the total portal flow.

#### 4. Discussion and conclusion

BCS is typically characterised by an occlusion of a major hepatic vein. This can be modelled as a much higher resistance in HV vasculature than normal. Through the presented computer model we have reproduced some subtle flow features which have been observed clinically. For example, Cazals-Hatem et al. studied pre-

transplantation BCS patients and reported that 94% of those (16 of 17) had reduced portal perfusion [6] but increased arterial flow, exactly as we have shown in Figure 5(a) and (b). This phenomenon can cause arterial hyperemia which may further contribute to the development of large regenerative nodules [6].

The circuit presented herein represents major improvements over the previous model of Ho et al. [7] in that the HABR effect is incorporated in both left and right lobes. Due to lack of in vivo measurements, we still had to estimate vasculatures parameters and impose boundary conditions from healthy livers, and assume these are unchanged in BCS [6]. This suggests that the simulations shown here are more likely to describe the initial flow changes resulting from BCS; and without further knowledge of how the vessel mechanics and geometry changes over time, further improvements in the model and flow analysis would be difficult.

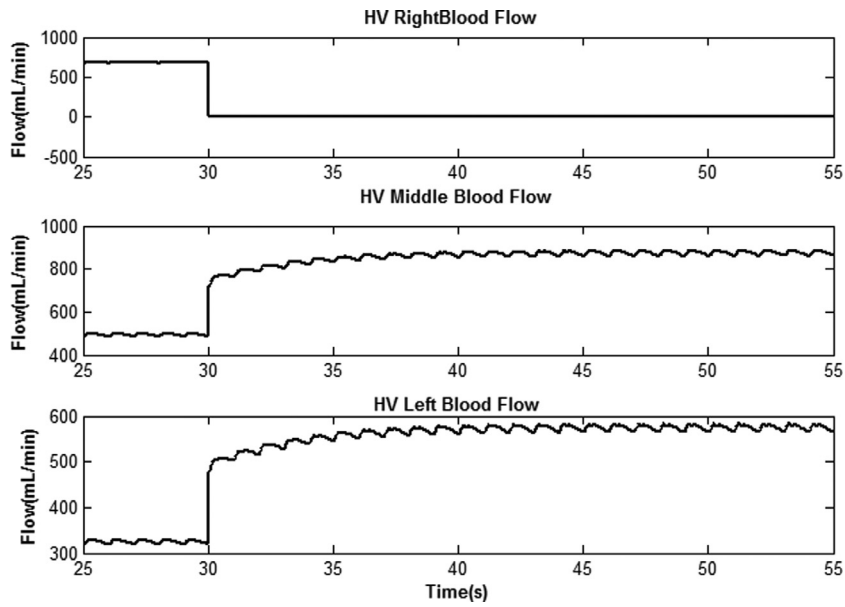


**Figure 4.** Flow drainage simulation after right HV occlusion: right HV flow was zero due to occlusion, yet flow in middle and left HV increased to mean 860 mL/min and 575 mL/min respectively.

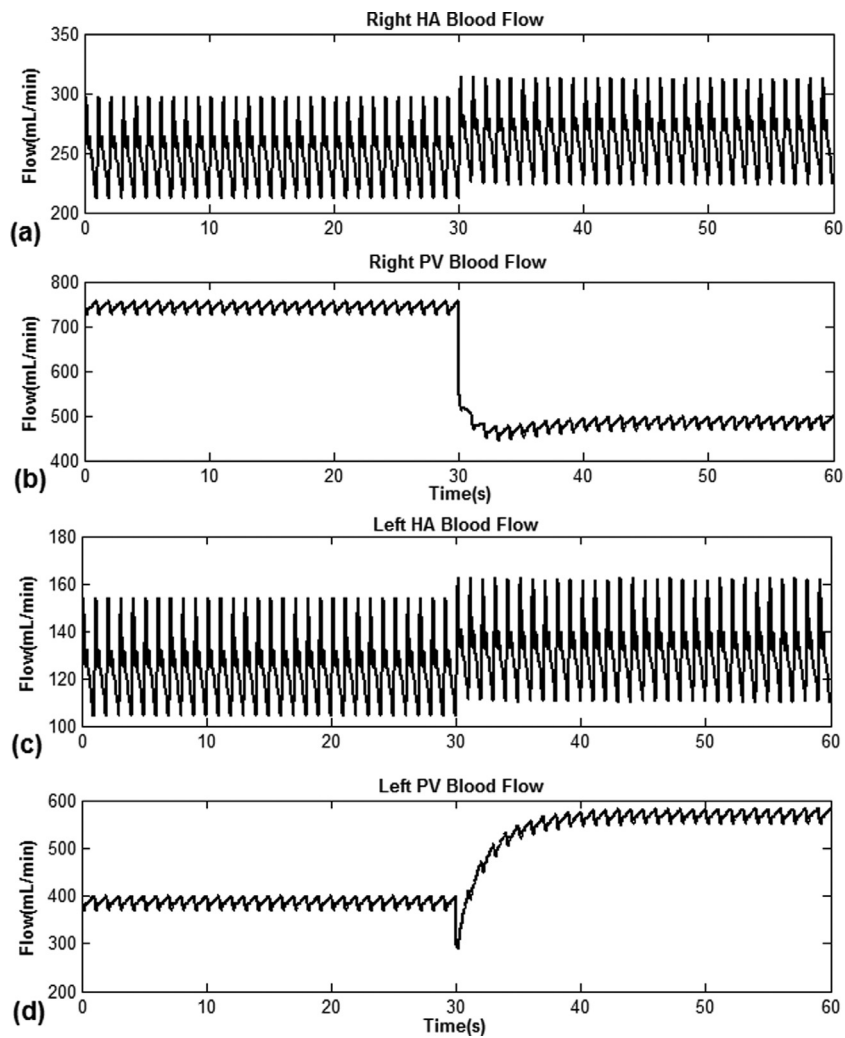


**Figure 5.** Blood supply to the left and right lobes after an acute occlusion of the right HV: (a) the right HA flow increases due to HABR whilst (b) the right portal flow drops sharply; (c) and (d) both left HA and PV flows increase to maintain the total hepatic flow.

It should be mentioned that although the present model was used for a typical BCS situation (right HV occlusion) it can also be adapted to other BCS cases, e.g. with different HV occlusion sites, by simply adjusting the circuit layout or parameters.

In conclusion, the first quantitative model for hepatic circulation under BCS has been introduced in this work. The proposed model serves as a reference for other studies of vascular disease in the liver.

### Competing interests

None declared.

### Funding

This work was supported by the [Auckland Medical Research Foundation](#) (Project number 3713305).

### Ethical approval

Not required.

### Supplementary materials

Supplementary material associated with this article can be found, in the online version, at doi:[10.1016/j.medengphy.2019.04.010](https://doi.org/10.1016/j.medengphy.2019.04.010).

### References

- [1] Menon KVN, Shah V, Kamath PS. The Budd–Chiari syndrome. *N Engl J Med* 2004;350:578–85. doi:[10.1056/NEJMra020282](https://doi.org/10.1056/NEJMra020282).
- [2] Selle D, Preim B, Schenk A, Peitgen H-O. Analysis of vasculature for liver surgical planning. *IEEE Trans Med Imaging* 2002;21:1344–57. doi:[10.1109/TMI.2002.801166](https://doi.org/10.1109/TMI.2002.801166).
- [3] Valla D-C. Budd–Chiari syndrome and veno-occlusive disease/sinusoidal obstruction syndrome. *Gut* 2008;57:1469–78. doi:[10.1136/gut.2007.133637](https://doi.org/10.1136/gut.2007.133637).
- [4] Mentha G, Giostra E, Majno PE, Bechstein WO, Neuhaus P, O’Grady J, et al. Liver transplantation for Budd–Chiari syndrome: a European study on 248 patients from 51 centres. *J Hepatol* 2006;44:520–8. doi:[10.1016/j.jhep.2005.12.002](https://doi.org/10.1016/j.jhep.2005.12.002).
- [5] Stanley P. Budd–Chiari syndrome. *Radiology* 1989;170:625–7.
- [6] Cazals-Hatem D, Vilgrain V, Genin P, Denninger M-H, Durand F, Belghiti J, et al. Arterial and portal circulation and parenchymal changes in Budd–Chiari syndrome: a study in 17 explanted livers. *Hepatology* 2003;37:510–19. doi:[10.1053/jhep.2003.50076](https://doi.org/10.1053/jhep.2003.50076).
- [7] Ho H, Sorrell K, Bartlett A, Hunter P. Modeling the hepatic arterial buffer response in the liver. *Med Eng Phys* 2013;35:1053–8. doi:[10.1016/j.medengphy.2012.10.008](https://doi.org/10.1016/j.medengphy.2012.10.008).
- [8] Lauth WW, Legare DJ, d’Almeida MS. Adenosine as putative regulator of hepatic arterial flow (the buffer response). *Am J Physiol – Heart Circ Physiol* 1985;248:H331–8.
- [9] Li T, Zhai S, Pang Z, Ma X, Cao H, Bai W, et al. Feasibility and midterm outcomes of percutaneous transhepatic balloon angioplasty for symptomatic Budd–Chiari syndrome secondary to hepatic venous obstruction. *J Vasc Surg* 2009;50:1079–84. doi:[10.1016/j.jvs.2009.06.049](https://doi.org/10.1016/j.jvs.2009.06.049).
- [10] Debbaut C, Monbaliu D, Casteleyn C, Cornillie P, Van Loo D, Masschaele B, et al. From vascular corrosion cast to electrical analog model for the study of human liver hemodynamics and perfusion. *IEEE Trans Biomed Eng* 2011;58:25–35. doi:[10.1109/TBME.2010.2065229](https://doi.org/10.1109/TBME.2010.2065229).
- [11] Marcos A, Olzinski A, Ham J, Fisher R, Posner M. The Interrelationship between portal and arterial blood flow after adult to adult living donor liver transplantation. *Transplantation* 2000;70:1697–703.
- [12] Eipel C, Abshagen K, Vollmar B. Regulation of hepatic blood flow: the hepatic arterial buffer response revisited. *World J Gastroenterol* 2010;16:6046–57. doi:[10.3748/wjg.v16.i48.6046](https://doi.org/10.3748/wjg.v16.i48.6046).